

## Optical Phonons in Mixed Sodium Potassium Tantalates

C. H. PERRY\* AND N. E. TORNBORG

*Spectroscopy Laboratory† and Research Laboratory of Electronics,‡ Massachusetts Institute of Technology, Cambridge, Massachusetts 02139*

(Received 10 January 1969)

The infrared and Raman spectra of members of the mixed-crystal system  $\text{Na}_x\text{K}_{1-x}\text{TaO}_3$  have been studied at temperatures from 4 to 600°K for  $x=0.0, 0.12, 0.40, 0.65,$  and  $0.85$ . The infrared data indicate that the low-frequency phonons are "soft" modes and are responsible for the ferroelectric phase change. The temperature dependence of the modes has been correlated with the dielectric behavior and is in agreement with current theories of displacive ferroelectrics. In the paraelectric phase, the Raman spectrum is entirely second order and qualitatively independent of cation concentration. First-order Raman bands are observed in the ferroelectric phase for  $x<0.70$  and a  $C_{4v}$  structure is strongly indicated. The frequencies of the optical modes at the center and at the boundary of the Brillouin zone have been deduced as a function of temperature and composition.

## INTRODUCTION

THE crystal  $\text{KTaO}_3$  has the cubic perovskite structure (symmetry group  $O_h$ ). X-ray data by Davis<sup>1</sup> which were obtained only at room temperature show that samples with concentrations from 0 to ~70%  $\text{NaTaO}_3$  remain cubic, with an almost linear decrease in lattice constant from 3.984–3.944 Å. Further increase in sodium content causes the lattice constants to decrease sharply and to show a well-defined  $c/a$  ratio. Initially, the structure becomes tetragonal, gradually shearing to pseudomonoclinic as the concentration approaches pure  $\text{NaTaO}_3$ .

The dielectric properties of  $\text{KTaO}_3$  have been investigated by Wemple<sup>2</sup> and indicate Curie-Weiss-law behavior with an extrapolated Curie temperature ( $T_C$ ) of 1–3°K. Davis<sup>1</sup> has obtained dielectric data of the mixed-crystal system  $\text{NaTaO}_3$ - $\text{KTaO}_3$  as a function of temperature.  $T_C$  rises with Na concentration to a maximum of 65°K for a sample with 48%  $\text{NaTaO}_3$ , falls with higher  $\text{NaTaO}_3$  concentrations, and becomes negative at ~72%  $\text{NaTaO}_3$ . The temperature-dependent dielectric constant undergoes a region of anomalous behavior in the midrange of Na composition as shown in Fig. 1. This has been interpreted by Davis<sup>1</sup> as a ferroelectric transition at the higher temperature, possibly followed by a phase transition to a tetragonal ( $C_{4v}$ ) structure at the lower temperature.

The cubic perovskites, with 5 atoms per unit cell, necessarily possess 15N degrees of freedom. Recourse to simple group theory<sup>3–5</sup> predicts that at the center of the

Brillouin zone these will consist of three triply degenerate infrared active (optic, symmetry  $F_{1u}$ ) modes, one triply degenerate infrared and Raman inactive (optic, symmetry  $F_{2u}$ ) mode, and one triply degenerate translational (acoustic, symmetry  $F_{1u}$ ) mode. A further consideration, however, is the existence of long-range electrostatic forces between the component ions.<sup>6,7</sup> These cause the boundary conditions for the longitudinal and transverse modes to differ,<sup>6</sup> thereby lifting the degeneracy of optic modes of  $F_{1u}$  symmetry.<sup>8</sup> Thus, the final description of the  $\mathbf{k}\approx 0$  phonon system of such crystals gives three doubly degenerate transverse optic modes and three nondegenerate longitudinal modes, one doubly degenerate transverse optic mode, which in turn is degenerate with a single longitudinal mode, and three acoustic modes (with  $\omega=0$ ).<sup>9</sup>

If the symmetry of the crystal is reduced to tetragonal ( $C_{4v}$  as in the case of  $\text{BaTiO}_3$  at room temperature<sup>10</sup>),

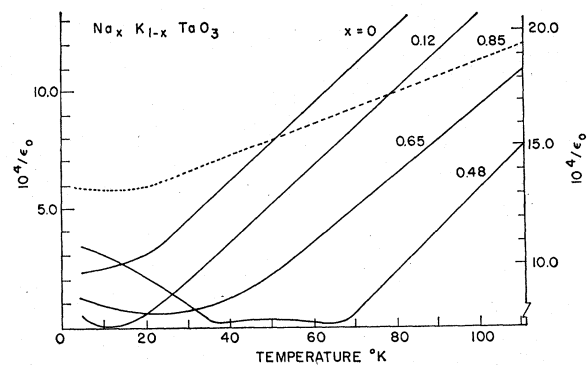


FIG. 1. Temperature dependence of the dielectric constant for  $\text{Na}_x\text{K}_{1-x}\text{TaO}_3$ , after Davis (Ref. 1). Dashed line corresponds to the right-hand scale.

<sup>6</sup> M. Born and K. Huang, *Dynamical Theory of Crystal Lattices* (Oxford University Press, London, 1962).

<sup>7</sup> R. Loudon, in *Advances in Physics*, edited by N. F. Mott (Taylor and Francis, Ltd., London, 1964), Vol. 14, p. 423.

<sup>8</sup> H. Poulet, *Ann. Phys. (Paris)* **10**, 908 (1955).

<sup>9</sup> R. A. Cowley, *Phys. Rev.* **134**, A981 (1964).

<sup>10</sup> F. Jona and G. Shirane, *Ferroelectric Crystals* (Pergamon Press, Inc., New York, 1963).

\* Present address: Department of Physics, Northeastern University, Boston, Mass. 02115.

† Laboratory supported in part by National Science Foundation Grant No. GP-4923.

‡ Work supported in part by the Joint Services Electronics Program, Contract No. DA28-043-AMC 02536(E) and by NASA Grant No. NGR 22-009-(237).

<sup>1</sup> T. G. Davis, S.M. thesis, Department of Electrical Engineering, MIT, 1965 (unpublished).

<sup>2</sup> S. H. Wemple, *Phys. Rev.* **137**, A1575 (1965).

<sup>3</sup> V. Heine, *Group Theory in Quantum Mechanics* (Pergamon Press, Inc., New York, 1960).

<sup>4</sup> J. T. Last, *Phys. Rev.* **105**, 1740 (1957).

<sup>5</sup> B. D. Silverman and G. K. Koster, *Z. Physik* **165**, 334 (1964).

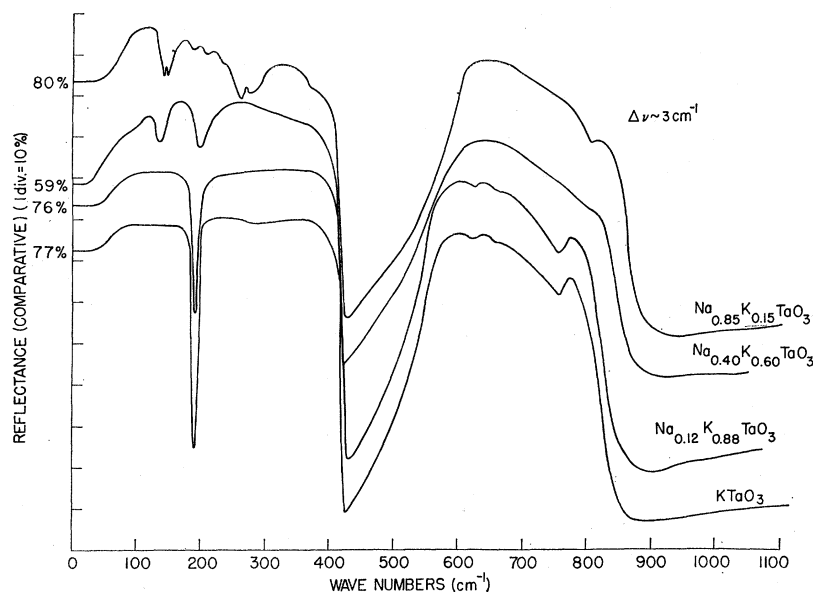


FIG. 2. Room-temperature reflectance spectra for four samples.

many of the above degeneracies are split and all modes become Raman active. The  $F_{1u}$  and  $F_{2u}$  modes separate into two distinct vibrations transforming as the  $A_1$  and  $E$ , and  $B_1$  and  $E$  irreducible representations of  $C_{4v}$ , respectively. The  $A_1$  and  $E$  modes are simultaneously infrared and Raman active whereas the  $B_1$  mode is only Raman active. Again, LO and TO modes which are degenerate by this description will be split by the long-range electrostatic field. In addition, the short-range forces cannot, in general, be considered isotropic and will result in further frequency splittings corresponding to differing phonon propagation directions. Using these considerations for tetragonal ( $C_{4v}$ )  $\text{BaTiO}_3$ , DiDomenico *et al.*<sup>11</sup> claim that 18 possible modes could be observed.

Miller and Spitzer<sup>12</sup> have studied the infrared active modes of pure  $\text{KTaO}_3$  at room temperatures by the reflectance technique, Perry and McNelly<sup>13</sup> have studied the lower-frequency modes as a function of temperature, and Nilsen and Skinner,<sup>14</sup> and Perry, Fertel, and McNelly<sup>15</sup> have studied its temperature-dependent Raman activity.

The principal objective of this research is the delineation of the phonon contributions to the various Raman bands. In the cubic phase, first-order (zone center) Raman transitions are forbidden but two-phonon combinations and overtones are allowed at all points in the Brillouin zone.<sup>7,16</sup> Thus, with the aid of neutron data on

the phonon dispersion curves<sup>17</sup> and such theoretical work as Cowley's,<sup>9</sup> average zone-boundary phonon frequencies may be estimated. This task is complicated by the large number of such phonon combinations which are possible. However, their density of states tends to be highest at the symmetry points of the Brillouin zone described by Boukaert and co-workers,<sup>16</sup> whose notation is used here. Thus, if  $N$  is the number of irreducible representations of the allowed vibrational modes which the group of the wave vector at a point in the Brillouin zone comprises, there are  $\frac{1}{2}N(N-1)$  summation bands,  $\frac{1}{2}N(N-1)$  difference bands, and  $N$  overtones. For perovskites, the symmetry points, with corresponding  $N$ 's, are  $\Gamma$  ( $k \approx 0$ ), 5;  $\Delta$ , 10;  $X$ , 10;  $\Sigma$ , 15;  $M$ , 11;  $\Lambda$ , 10;  $R$ , 6.<sup>9</sup> Since current neutron data are available only for  $\Delta$  and  $X$ , estimates must be restricted to those. The possible contributions to a given Raman band may be further restricted by noting the behavior of intensity and frequency under temperature variation, and frequency with mass variation. Also of interest is the nature of the phase change itself and the behavior of the "soft" ferroelectric mode. This behavior seems to correspond quite well with the calculations of Anderson,<sup>18</sup> Cochran,<sup>19</sup> and Nakamura,<sup>20</sup> and thus is important in the verification of the theory of displacive ferroelectrics.

The reduction in symmetry, which occurs for Na concentration greater than 70% and in the ferroelectric phase, allows all modes to become Raman active at  $\Gamma$  (zone center). This affords the opportunity to examine

<sup>11</sup> M. DiDomenico, Jr., S. H. Wemple, S. P. S. Porto, and R. P. Bauman, *Phys. Rev.* **174**, 522 (1968).

<sup>12</sup> R. C. Miller and W. G. Spitzer, *Phys. Rev.* **129**, 94 (1963).

<sup>13</sup> C. H. Perry and T. F. McNelly, *Phys. Rev.* **154**, 456 (1967).

<sup>14</sup> W. G. Nilsen and J. G. Skinner, *J. Chem. Phys.* **47**, 1413 (1967).

<sup>15</sup> C. H. Perry, J. H. Fertel, and T. F. McNelly, *J. Chem. Phys.* **47**, 1619 (1967).

<sup>16</sup> L. P. Boukaert, R. Smoluchowski, and E. Wigner, *Phys. Rev.* **50**, 58 (1936).

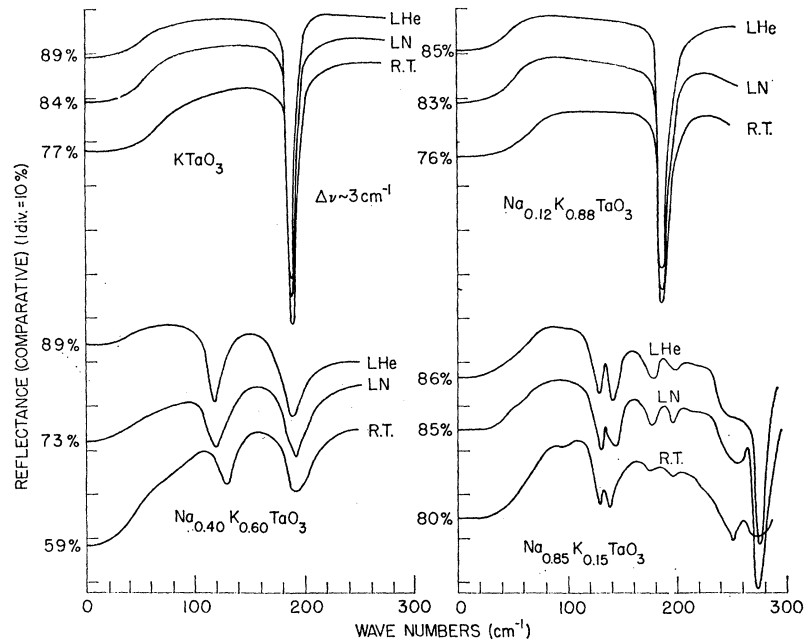
<sup>17</sup> G. Shirane, R. Nathans, and V. J. Minkiewicz, *Phys. Rev.* **157**, 396 (1967).

<sup>18</sup> P. W. Anderson, in *Fizika Dielektrikov*, edited by G. I. Skanavi (Akademiya Nauk SSSR Fiz., Moscow, 1960).

<sup>19</sup> W. Cochran, in *Advances in Physics*, edited by N. F. Mott (Taylor and Francis, Ltd., London, 1960), Vol. 9, p. 387.

<sup>20</sup> T. Nakamura, *Inst. Solid State Phys., Tokyo A186*, 1 (1966); *J. Phys. Soc. Japan* **21**, 491 (1966).

FIG. 3. Low-frequency reflectance spectra as a function of sample and temperature.



the phase change directly and to verify that the spectrum in the cubic phase is indeed second order.

### EXPERIMENT

The  $\text{Na}_x\text{K}_{1-x}\text{TaO}_3$  crystals used had  $x=0, 0.12, 0.40, 0.65,$  and  $0.85$  and were grown by the method used by Wemple,<sup>21</sup> modified as described by Davis.<sup>1</sup> They were cut and polished to square plates approximately  $1 \times 6 \times 6$  mm with the  $\{100\}$  planes in the surfaces.

The infrared reflectance measurements below  $250 \text{ cm}^{-1}$  were made with the Michelson interferometer<sup>22</sup> used by Perry and McNelly.<sup>18</sup> At higher frequencies, a Perkin-Elmer model-521 grating instrument was used. Temperature control was achieved through the use of an ordinary cold-tail Dewar.

The Raman studies were made on a Cary model 81 with He-Ne laser excitation and right-angle scattering with  $X(ZZ)Y$  symmetry,  $X, Y,$  and  $Z$  lying in the  $\langle 100 \rangle$  directions in the sample. Symmetry changes to  $X(YZ)Y$  and  $X(YX)Y$  did not make important qualitative changes and merely reduced line intensity uniformly. Temperature control at lower temperatures in this case was obtained with a continuous gas transfer Dewar with quartz windows. The cold gas was obtained either by passing nitrogen through a coil immersed in a dry-ice-acetone bath or liquid nitrogen in a Dewar, or by transferring gas boiled off by power dissipated in liquid helium. By suitable gas flow and heat-shielding modi-

fications, this procedure allowed temperature control to less than a degree within the regions 8–50, 77–120, 210–300°K. The temperature was monitored by a precisely calibrated doped germanium 4-wire resistance thermometer and by a copper-constantan thermocouple, both of which were mounted on the small bracket that held the sample. Elevated temperatures were obtained with a Variac-controlled 40-Wheating element on which the sample was mounted with a copper bracket, inside an enclosure to restrict convection but not conduction or radiation. These temperatures were monitored with the copper-constantan thermocouple. Temperature control with this arrangement was  $\pm 5^\circ\text{K}$ .

### RESULTS

Continuous reflection spectra were obtained by normalizing the data of the interferometer to those of

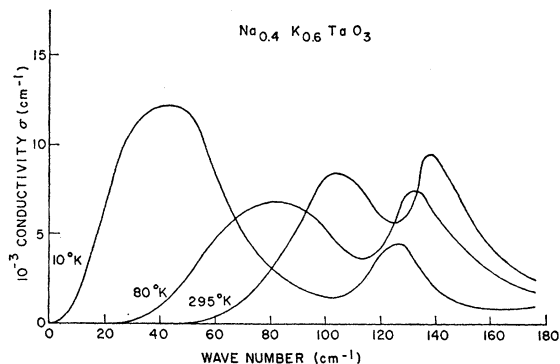


FIG. 4. Low-frequency conductivity derived from KK analysis of the reflectance spectra.

<sup>21</sup> S. H. Wemple, Ph.D. thesis, Department of Electrical Engineering, MIT, 1963 (unpublished); Technical Report No. 425, Research Laboratory of Electronics, MIT, Cambridge, Mass., 1964 (unpublished).

<sup>22</sup> C. H. Perry, R. Geick, and E. F. Young, Appl. Opt. 5, 1171 (1966).

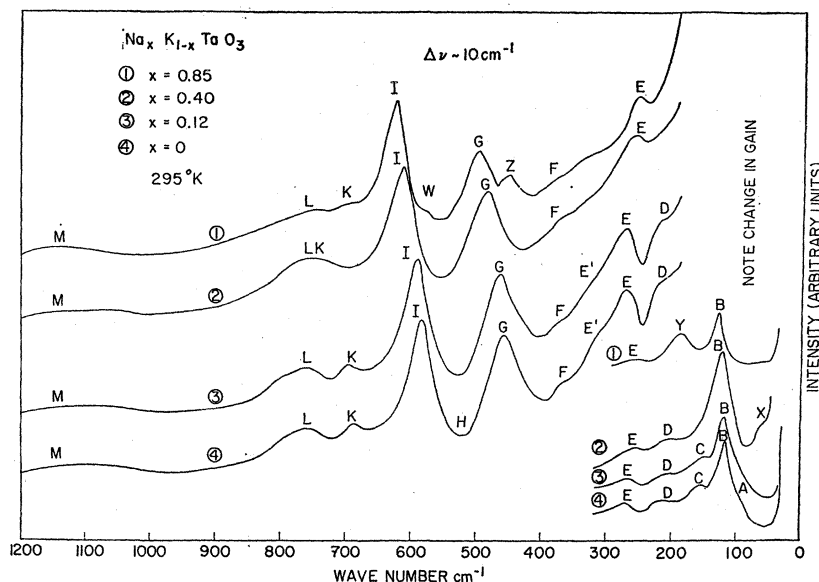


FIG. 5. Room-temperature Raman spectra of four samples.

the grating spectrometer. This was done by comparing the two data sets in the spectral region covered by both instruments, and resulted in consistent values for the reflectance maxima at low frequency. The extrapolated "dc" reflectivities obtained from this procedure also compared favorably with those calculated from Davis's<sup>1</sup> dielectric constant data. Examples of these spectra at room temperature are presented in Fig. 2, while the low-frequency data of samples at various temperatures appear in Fig. 3. Each of the details in Fig. 3 is the result of the average of at least two interferometer runs, and of as many as six. These reflectance spectra were subjected to a Kramers-Kronig (KK) analysis,<sup>23,24,12</sup> to obtain the real and imaginary parts of the dielectric constant ( $\epsilon'$  and  $\epsilon''$ ) and the reciprocal dielectric constant ( $\eta'$  and  $\eta''$ ), the conductivity ( $\sigma = \frac{1}{2}\epsilon''\nu$ ), and the resistivity ( $\rho = 2\eta''/\nu$ ). A representative series of low-frequency conductivities is presented in Fig. 4.

The Raman spectra are the average of several retracings of the regions of interest. Room-temperature results for most samples are presented in Fig. 5, while Fig. 6 shows the results for the entire temperature range for the sample nearest midrange of composition.

The Cary 81 is capable of running with either the conventional single slit or with a double slit for greater signal. The latter is usable only above  $\sim 200\text{ cm}^{-1}$ . This accounts for the appearance of the Raman spectra presentation, the lower intensity plots below  $300\text{ cm}^{-1}$  being single-slit results, and the remainder double-slit results. No effort has been made to renormalize one or the other of these for purposes of presentation, since the current form is considered more indicative of the quality of the results obtained.

## DISCUSSION

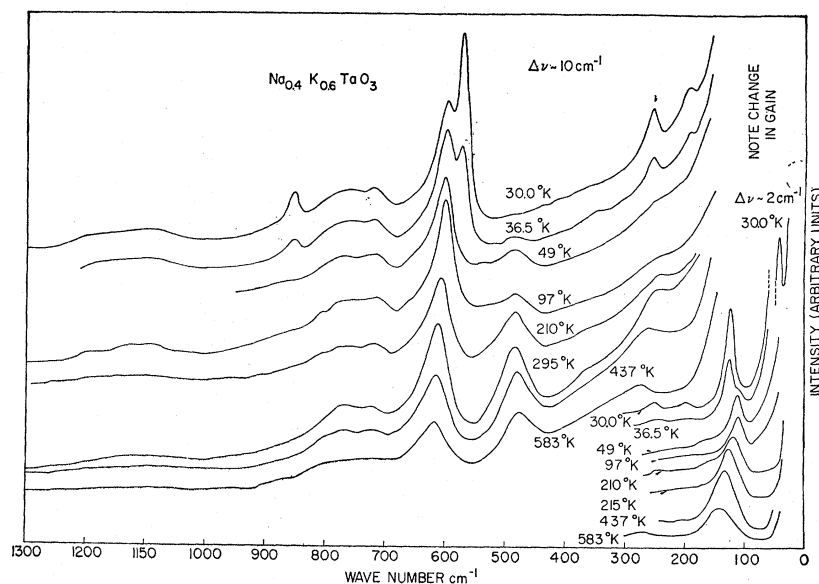
The infrared studies provide the frequencies of the independent first-order lattice modes and establish a starting point for the Raman work. In Fig. 2, the large dip, which occurs between  $450$  and  $550\text{ cm}^{-1}$ , corresponds to the highest-frequency transverse optic mode ( $\text{TO}_4$ ), the shoulder at the left to the lowest mode ( $\text{TO}_1$ , the "soft" mode), and for the two with the lowest percent of Na composition the dip between  $190$  and  $200\text{ cm}^{-1}$  corresponds to the next highest mode ( $\text{TO}_2$ ). Proceeding to the reflectance spectra for the two samples with the highest percent of sodium, however, one can see that the reduction in lattice symmetry becomes visible through the splitting of previously obtained lines, and the introduction of new ones. For the  $\text{Na}_{0.40}\text{K}_{0.60}\text{TaO}_3$  sample the  $\text{TO}_2$  mode displays "two-mode" behavior<sup>25</sup> with the introduction of the lower-frequency mode at approximately  $138\text{ cm}^{-1}$ . As one proceeds to higher concentrations of Na, the relative strengths of these two lines change, with their integrated intensities varying approximately in the same ratio as the ratio of the Na to the K concentration. Further splitting of these lines occurs in the  $\text{Na}_{0.85}\text{K}_{0.15}\text{TaO}_3$  sample where the structure is orthorhombic.<sup>1,10</sup> In addition, the previously degenerate and infrared-silent  $\text{LO}_2:\text{TO}_3$  modes (formerly of  $F_{2u}$  symmetry) are visible in this sample in the region  $210\text{--}280\text{ cm}^{-1}$ . These low-frequency details and their temperature dependence may be seen more clearly in Fig. 3. The frequencies of the active TO modes may be obtained from the maxima of the conductivity and the frequencies of the corresponding LO modes from the

<sup>23</sup> T. S. Robinson, Proc. Phys. Soc. (London) **B65**, 910 (1952).

<sup>24</sup> C. H. Perry, R. N. Khanna, and G. Rupprecht, Phys. Rev. **135**, A408 (1964).

<sup>25</sup> G. Lucovsky, M. Brodsky, and E. Burstein, in *Localized Excitations in Solids*, edited by R. F. Wallis (Plenum Press, Inc., New York, 1968), p. 592.

Fig. 6. Temperature-dependent Raman spectrum of  $\text{Na}_{0.40}\text{K}_{0.60}\text{TaO}_3$ .



peaks in the resistivity.<sup>26,27</sup> These are the frequencies shown in Table I. The conductivity and resistivity give the upper and lower bounds on their respective frequencies for materials exhibiting single-mode behavior (or having isolated TO-LO frequency pairs).<sup>28</sup> For materials with relatively small damping of the optic modes, however, the differences between the upper bound, lower bound, and the actual frequency are quite small. The materials examined in this work meet the above criteria; the expected deviations in frequency from the values given are much less than the experimental error ( $\pm 5 \text{ cm}^{-1}$  for frequencies greater than about  $40 \text{ cm}^{-1}$ ).

Cochran predicts that the frequency dependence of the soft mode should be  $\omega^2 \propto (T - T_c)$ .<sup>17</sup> This holds quite well within the experimental error above the Curie temperatures of the samples with  $x=0, 0.40,$  and  $0.85$ . However, none of the bands labeled  $\text{TO}_1$  agree with the predicted frequency dependence for soft-mode behavior for the samples 0.12 and 0.65. Using Davis's dielectric data<sup>1</sup> and assuming that the Lyddane-Sachs-Teller (LST) relation can be applied to these mixed-crystal systems, both the 0.12 and 0.85 samples predict frequencies that are considerably lower than those observed and shown in Table I. The experimental error in the frequency measurement determined from the infrared reflectance data may be as much as  $\pm 10 \text{ cm}^{-1}$  for frequencies less than about  $30 \text{ cm}^{-1}$ . However, the values observed in the Raman measurements in the ferroelectric phase are still high and it is possible that

these bands are not the soft modes normally referred to in the perovskites but are the higher of soft-mode pairs displaying two-mode behavior similar to  $\text{TO}_2$  mentioned above.

Figures 5 and 6 are representative of the Raman spectra obtained, and correspond to the diagonal elements of the Raman tensor. The most important feature to be noticed in Fig. 5 is the close correspondence between the Raman spectra as the  $\text{NaTaO}_3$  concentration is varied. The frequency change is quite gradual, relative intensities remain the same, and for the most part no new frequencies occur. We take this to mean that while the unit cell cannot be strictly the same in each case, nevertheless there must exist a pseudo-Brillouin zone which qualitatively varies very little as the composition is varied. This is confirmed by the room-temperature x-ray measurements on these materials.<sup>1</sup> One may expect the changes in frequencies associated with the phonon system to arise from the average mass change and the average change in lattice constant. The first-order frequencies obtained in this study, however, cannot be correlated directly with those expected from variations in the reduced mass, and the nature of the anharmonicity of the lattice vibrations would have to be known to deal with the relation between frequency and lattice constant. We are thus limited to the conclusion that the assignments of the phonon contribution to the various bands are consistent from one composition to the next. The final points of interest in Fig. 5 are the bands marked  $W, Z, Y$  on the spectrum for 85%  $\text{NaTaO}_3$ . These are interpreted as the  $\text{TO}_4, \text{LO}_3,$  and  $\text{LO}_1$  or  $\text{TO}_2$  at zone center that become Raman active because of the reduction in symmetry with increasing  $\text{NaTaO}_3$  percentage mentioned above.

For the two samples with the highest Curie temperatures (40%  $\text{NaTaO}_3$ ,  $T_c = 55^\circ\text{K}$ ; 65%  $\text{NaTaO}_3$ ,  $T_c$

<sup>26</sup> F. Seitz, *Modern Theory of Solids* (McGraw-Hill Book Co., New York, 1940), Chap. XVII, p. 635.

<sup>27</sup> A. S. Barker, Jr., in *Infrared Behavior of Ferroelectric Crystals, Ferroelectricity*, edited by E. F. Weller (Elsevier Publishing Co., Amsterdam, 1967).

<sup>28</sup> J. F. Parrish, Ph.D. thesis, Department of Physics, MIT, 1969 (unpublished).

TABLE I. Frequencies of the TO and LO phonon modes for  $\mathbf{k} \approx 0$ .

Sample	KTaO <sub>3</sub>					Na <sub>0.12</sub> K <sub>0.88</sub> TaO <sub>3</sub>			Na <sub>0.40</sub> K <sub>0.60</sub> TaO <sub>3</sub>				Na <sub>0.65</sub> K <sub>0.35</sub> TaO <sub>3</sub>					Na <sub>0.85</sub> K <sub>0.15</sub> TaO <sub>3</sub>						
Temperature (°K)	463	295	232	126	12	295	80	10	295	80	30	10	295	80	21	10	10	295	295	109	80	24	10	
Type	IR	IR	IR	IR	IR	IR	IR	IR	IR	IR	R	IR	IR	IR	R	IR	R	IR	R	R	IR	R	IR	
	No first-order Raman down to 5°K. No ferroelectric transition					No first-order Raman down to 30°K. $T_C \approx 15^\circ\text{K}$			No first-order Raman observed down to 37°K. $T_C \approx 37^\circ\text{K}$				$T_C \approx 35^\circ\text{K}$					No ferroelectric transition						
TO <sub>1</sub>	106	88	79	58	25	75	50	48	102	81	42	39	72	51		75	75		70	66	65	57		
LO <sub>1</sub>	184	184	184	184	183	186	183	183	186	186		186	192				132		130	132	130	132		
						150		156	138	132	128	129	138	132	137	132	136	144			147	150	147	
TO <sub>2</sub>	199	199	198	198	196	198			198	198	204	201	200	198	198	204		204	195		195	205	195	195
															225				225		216	216	219	219
LO <sub>2</sub> /TO <sub>3</sub>									255						253		250	255	255	246	246	261	261	
LO <sub>3</sub>		421	421	421	421	420	420	420	414	414		414	408	410			414		450	414	450	414		
TO <sub>4</sub>	547	547	547	547		540	540	540	576	573	572	570	585	582	579	582	578	584		584	580	584	584	
LO <sub>4</sub>	838	838	838	837		819	819	819	849	849	850	849	864	864	862	864	862	864		864	864	864	864	

= 35°K), sharp peaks arise at the lowest temperatures at approximately 42, 128, 200, 255, 572, and 850 cm<sup>-1</sup> for the former and at 137, 253, 579, and 862 cm<sup>-1</sup> for the latter. Examples of the Raman spectra of Na<sub>0.40</sub>K<sub>0.60</sub>TaO<sub>3</sub> at various temperatures may be seen in Fig. 6. These peaks are interpreted as first-order Raman lines and are in good agreement with the bands seen in the infrared as shown in Table I. The appearance of a first-order Raman spectrum is presumed caused by a lowering of the symmetry of the crystal and in the case of 40% NaTaO<sub>3</sub> this can be seen to occur at approximately the same temperature as the lower-temperature minimum of the 1/ε plot in Fig. 1. There is no evidence for the existence of these lines at temperatures of 49°K and higher for the 40% NaTaO<sub>3</sub> sample and this indicates the probable lack of any symmetry change to C<sub>4v</sub> at the 55°K Curie temperature. The behavior of the Raman spectra of the Na<sub>0.65</sub>K<sub>0.35</sub>TaO<sub>3</sub> sample is qualitatively similar but exhibits no sharp low-frequency line above 30 cm<sup>-1</sup>. Also, the dielectric constant of this sample possesses no anomalous behavior and the apparent phase transition (at ~35°K) is approximately at the Curie temperature.

The infrared and Raman studies must meet several requirements to be used most successfully with the available x-ray data in limiting the possible lattice symmetries. The Raman investigations must distinguish between the various polarizations of incident and scattered light. Lack of uniformity in the polarization of the crystal defeated these measurements. The observed half-widths of the lines must be sufficiently small to allow the possible splittings to be seen. In both the Raman and infrared, the instrumental half-widths were substantially less than the width of the observed lines, but no splitting attributable to crystal anisotropy could be detected with the exception of the sample with the

highest Na concentration. Therefore, the mixed crystals must have a structural symmetry which allows no splitting, or one in which the splitting is smaller than the linewidths observed. In either case, it is impossible to discern the crystal's symmetry on the basis of line multiplicity.

The highest symmetries which permit a permanent dipole moment to exist are C<sub>4v</sub> and C<sub>6v</sub>. A structure with C<sub>6v</sub> symmetry would require the TaO<sub>3</sub> octahedra to be linked in quite a different manner from the cubic perovskite structure and the phonon frequencies of the two phases could be expected to differ considerably. This difference is not observed. Thus, the most reasonable assumption to make regarding the symmetry of the ferroelectric phase is C<sub>4v</sub>, similar to a large number of other perovskite ferroelectrics.

Because of the mode splitting and infrared and Raman activity required by C<sub>4v</sub> symmetry and explained above, the assumption must be made that the splittings involved are smaller than the linewidths observed (this would be necessary for C<sub>6v</sub> also). The further assumption must be made that the former F<sub>2u</sub> mode is too weakly coupled to a dipole moment to be seen in the infrared. This is found to be true for a wide variety of perovskites, in particular BaTiO<sub>3</sub>,<sup>11</sup> so it seems justified here. Further consideration of more complex space groups has not been made since the data presented here is considered insufficiently detailed to provide the information that would be necessary.

One requirement of a second-order transition is that any distortion involved, leading to a structure of lower symmetry, evolve continuously from a value of zero at the transition temperature.<sup>20</sup> A small departure from a high symmetry toward a lower one will result in a

<sup>20</sup> C. Haas, Phys. Rev. **140**, 863 (1965).

correspondingly small introduction of interactions characteristic of just the lower one. Therefore, the features belonging to the lower of two symmetries separated by a second-order transition will develop comparatively slowly as the temperature becomes less than that of the transition. A slowly growing first-order Raman spectrum is thus a necessary, although not sufficient, condition for a second-order transition to exist between a phase in which first-order Raman processes are forbidden and one where they are not. Indeed, the advent of the first-order lines in the work presented here is quite gradual, the intensities of the lines growing by an order of magnitude over a temperature range of several degrees. This behavior is independent of the previous state of the crystal and apparently involves no lower bound on the first-order line intensity. Since there is a complete lack of evidence indicating a first-order transition at the Curie temperature, this makes it seem reasonable to presume that the transition is second order. This further enforces the supposition that  $C_{4v}$  is the symmetry of the ferroelectric phase. Following this, and further assuming that a phase change is involved at the point of anomalous behavior of the dielectric constant, the symmetry of this intermediate phase must be  $D_{4h}$ . This result is compatible with the spectra observed under the assumptions we have already had to make regarding mode splitting and infrared activity since under  $D_{4h}$  symmetry the  $F_{1u}$  mode becomes  $A_{2u} + E_u$  and the  $F_{2u}$  mode becomes  $B_{2u} + E_u$ . All are infrared active, none are Raman active.

In considering the splitting observed in the sample with highest Na composition, it seems reasonable to presume that the unit cell has been doubled in the  $c$  direction. This would conform with reports of the structure of pure  $\text{NaTaO}_3$ .<sup>10</sup> Davis conjectures that the structure varies continuously from  $C_{4v}$  to that of  $\text{NaTaO}_3$  in the composition range above 80% Na. The structural symmetry of  $\text{Na}_{0.85}\text{K}_{0.15}\text{TaO}_3$  must then transform as the group  $C_{2v}$  or a related space group as a consequence of the above discussion. This implies that all modes are triply split and Raman active, all but one being infrared active as well. Such splitting is indeed seen in the Raman at low temperatures for the former  $F_{2u}$  mode but interpretation is a trifle obscure if the unit cell can possibly be doubled. It is quite unlikely that any of the actual splitting observed is due to a relaxation of selection rules due to the destruction of translational symmetry because of the distribution of the different species K and Na. If this distribution is entirely random, one expects the matrix elements corresponding to momentum nonconservation to be independent of  $\Delta k$  and functions of  $x$  only (where  $x$  is the percentage composition of Na). This dependence upon  $x$  would be symmetric about  $x=0.5$  and would have a maximum there. Clustering of the species would have to be quite drastic to alter this description significantly. No real difference can be seen between the shapes of the first-order Raman lines of samples for  $x=0.4$  and  $x=0.85$  at similar

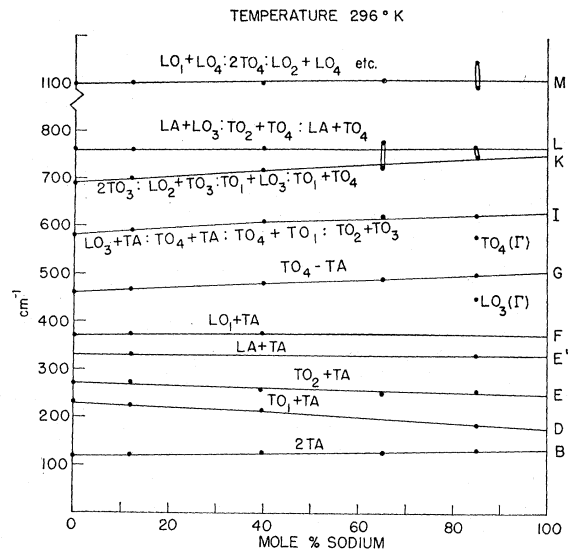


Fig. 7. Phonon combination assignment and their frequency dependence on composition. Letters at right correspond to peak labels in Fig. 5.

temperatures. Also, the shape of each infrared line remains similar from sample to sample at a given temperature. These facts are taken as a justification for ignoring the possible effects of random momentum nonconservation.

In Fig. 7, frequencies of the Raman bands are plotted as a function of composition. The letters at the right of the plot correspond to the letters identifying peaks in the spectra of Fig. 5. The corresponding plot of frequencies for all compositions as a function of temperature occurs in Fig. 8.

Except as noted in the figures, each band is the result of second-order processes within the material. Although the magnitudes of the photon wave vectors are negligible compared to the size of the Brillouin zone, momentum conservation does not exclude those processes involving, for instance, two phonons of equal and opposite wave vector. Phonons distributed throughout the Brillouin zone can thus contribute to higher-order processes. In general, the principal determinants of scattered intensity will be the product of the density of states of the phonons taking part and the coupling of these phonons to the radiation. The sum or difference of the phonon frequencies determines the Raman frequency shift. As noted in the Introduction, the number of these processes which are available is rather large, and their group theoretical selection rules are quite lenient. Thus, a restrictive explanation of the various Raman bands in terms of phonon contributions requires careful interpretation of the experimentally discovered dependence of frequency and intensity on temperature and composition.

The shapes of the second-order bands change very little as a function of composition, and tend merely to

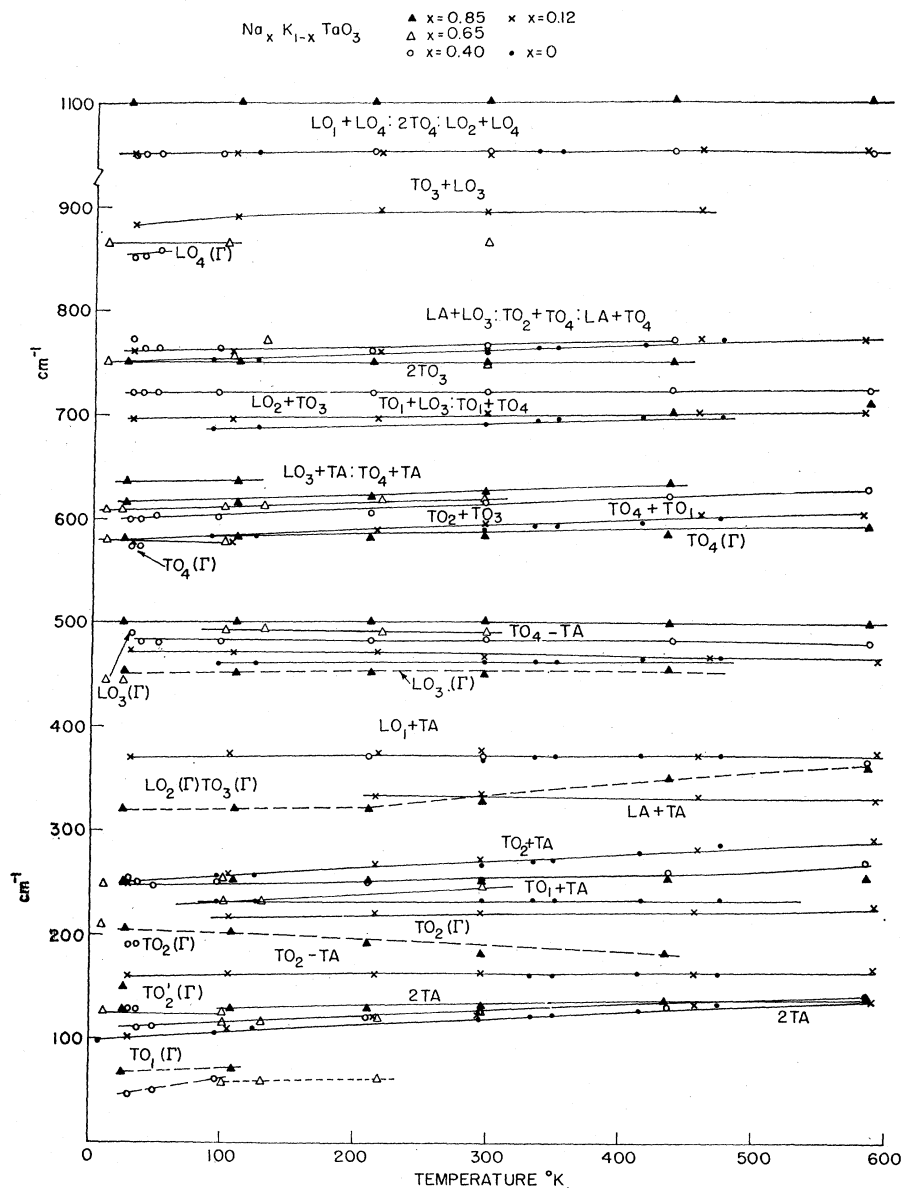


FIG. 8. Complete tabulation for all compositions of phonon combination frequency versus temperature.  $\Gamma$  refers to single phonons with  $k \approx 0$ .

become sharper with decreasing temperature. Since the density of states varies considerably throughout the Brillouin zone, and since the shape of a second-order band can generally be attributed to this variation,<sup>30</sup> the likelihood is high that a given distinctive peak in the Raman scatter is caused by phonons in a fairly narrow region of the zone. Therefore, the supposition is justified that the frequencies chosen for the various second-order processes represent these processes over narrow regions of the zone if one can consistently make unambiguous selection of frequency on the basis of the distinctive band shapes.

<sup>30</sup> E. Burstein, in *Phonons and Phonon Interactions*, edited by T. A. Bak (W. A. Benjamin, Inc., New York, 1964), p. 276.

The temperature and composition dependence of the phonon dispersion curves will, in general, be due to that of the linear lattice force constants, the electrostatic restoring force, and the phonon self-energy (i.e., the anharmonic portion). Without a detailed understanding of each of these, one has no assurance that the behavior of the dispersion curve as a function of temperature and composition will be uniform from the center to the edge of the zone. The dependence of the frequencies of second-order bands on temperature and composition is a sum of the individual phonon dispersion curves weighted by the density of states of their partners in the combination process. For this reason, the temperature dependence of the frequency of a given overtone band could be



TABLE II. Assignments of the phonon mode and their average frequencies at the zone boundaries based on Figs. 7 and 8.

Na(%) Temperature (°K) Mode	12						40						65				85							
	30	110	214	295	458	591	30	36.5	49	97	210	296	437	583	100	130	218	295	33	109	210	296	433	586
TA	50	55	58	60	65	67	55	55	56	57	60	62	66	70	58	59	61	63	64	65	66	66	67	69
LA			277	272	263	258																		
TO <sub>1</sub>		160	159	159	157																			
LO <sub>1</sub>	320	315	312	310	305	303	315	315	314	313	310	308	304	300										
TO <sub>2</sub>	200	200	204	208	213	220	200	197	191	191	190	192	192	195	175	175	181	184	183	183	184	185	186	185
TO <sub>4</sub>	522	525	527	528	531	531	539	539	540	540	541	542	545	548	552	553	553	556	564	565	566	565	564	565

positive, for instance, while the temperature-dependent contribution of this phonon to some other combination process could be negative. If, however, it is assumed that the principal scatter results from processes within small portions of the Brillouin zone, inferences can be drawn regarding the temperature- and composition-dependent frequency contribution of various phonons to the bands observed. This procedure has been used here. Reasonable agreement with neutron data noted by Perry *et al.*,<sup>13</sup> who followed a similar analysis, indicates the validity of these assumptions. The neutron data were available only for points  $\Delta$  and  $X$  in the Brillouin zone and the agreement with Raman results implies, therefore, that processes at these points are the predominant causes of the inelastic scattering observed. This supposition is substantiated considerably by the fact that there is negligible change in the second-order spectrum upon the ferroelectric phase change. If this change does indeed involve a transition to  $C_{4v}$  symmetry, the group of the wave vector at  $\Delta$  does not change at all and that at  $X$  loses only the inversion. Thus, these two points, with their associated selection rules, are least affected and contributions from processes with wave vectors located there will remain approximately constant.

The temperature dependence of the band intensities may also be used to discriminate between summation and difference processes. If  $\omega_j$  and  $\omega_k$  are two phonon frequencies, then the dependence of the intensities of the

two processes on phonon occupation numbers is

$$\omega_j + \omega_k \leftrightarrow 1 + n_j + n_k + n_j n_k,$$

$$\omega_j - \omega_k \leftrightarrow n_j n_k + n_k,$$

where  $n_j$ ,  $n_k$  are the respective occupation numbers given as a function of temperature by Bose statistics.<sup>30</sup> Thus as temperature is lowered, a difference process will disappear while a summation process will approach a constant integrated intensity.

These studies allow one to deduce the "average" behavior of individual phonons near the zone boundary. The conclusions reached are probably applicable to a very limited number of points near the boundary. Table II lists those frequencies which have been determined. The assignments have been based on the work of Perry, Fertel, and McNelly,<sup>15</sup> and of Nilsen and Skinner<sup>14</sup>; both of these in turn depended on the neutron work of Shirane, Nathans, and Minkiewicz<sup>17</sup> for the assignment of the low-frequency modes.

#### ACKNOWLEDGMENTS

We would like to acknowledge the cooperation of Dr. T. G. Davis, Materials Center, MIT, in providing the samples and participating in certain aspects of this work. This work constitutes a portion of the doctoral thesis of one of us (N. E. T.) to be submitted to Physics Department, MIT, in partial fulfillment of the requirements for the Ph.D. degree.